

Stability of periodic traveling waves in the Aliev–Panfilov reaction–diffusion system



M. Osman Gani^{a,b,*}, Toshiyuki Ogawa^b

^a Meiji Institute for Advanced Study of Mathematical Sciences, Meiji University, 4-21-1 Nakano, Nakano-ku, Tokyo 164-8525, Japan

^b Graduate School of Advanced Mathematical Sciences, Meiji University, 4-21-1 Nakano, Nakano-ku, Tokyo 164-8525, Japan

ARTICLE INFO

Article history:

Received 13 March 2015

Revised 17 August 2015

Accepted 1 September 2015

Available online 10 September 2015

Keywords:

Periodic traveling wave

Aliev–Panfilov model

Eckhaus instability

Oscillating periodic traveling wave

Essential spectrum

ABSTRACT

We study the two-component Aliev–Panfilov reaction–diffusion system of cardiac excitation. It is known that the model exhibits spiral wave instability in two-dimensional spatial domains. In order to describe the spiral wave instability, it is important to understand periodic traveling wave instability resulting from the model. We determine the existence and stability of periodic traveling waves in the model. In addition, we calculate the stability boundary between stable and unstable periodic traveling waves in a two-dimensional parameter plane. It is observed that the periodic traveling waves express instability by a stability change of Eckhaus type. As a result, a stable wave bifurcates to an oscillating periodic traveling wave. We describe these phenomena by calculating the essential spectra of the waves. Furthermore, we study the stability of the waves as a function of the gaps between two nullclines. In two dimensions, we determine the spiral wave instability based on the stability boundary of the periodic traveling waves.

© 2015 Elsevier B.V. All rights reserved.

1. Introduction

A periodic traveling wave (PTW) solution is an important solution pattern in one dimension for many partial differential equations (PDEs) in nonlinear systems. Periodic traveling wave solutions (PTWs) were first studied in 1973 by Kopell and Howard, who used coupled reaction–diffusion equations for oscillatory systems [1]. They showed that waves with sufficiently low amplitude are always unstable whereas those with sufficiently high amplitude are always stable. PTWs have also been observed in biological [2–4], physical [5–7], chemical [8–10] and ecological systems [11–13]. These are often modeled using a two-component reaction–diffusion system of equations, e.g., [1,14–17]. The determination of PTW instability for excitable media is important for researchers owing to the complex spatiotemporal patterns exhibited by the instability. A powerful and standard method for studying the PTWs of PDEs is the method of continuation [18]. In this paper, we study the stability of PTWs numerically by using a two-component excitable reaction–diffusion system for cardiac cell dynamics [19]. The first and most widely used PDE model is the FitzHugh–Nagumo (FHN) model, which was developed by FitzHugh and Nagumo [14,15]. The FHN model is a simplified version of the Hodgkin and Huxley model [20], a four-variable (V , m , n , and h) ionic model that describes the fast-slow dynamics of an excitable system of a spiking neuron. Previous studies of PTWs focused on ionic models [21–23] and PDE models for excitable systems [17,24–26] and other systems [27–29]. The Aliev–Panfilov model, which is a modified version of the FHN model,

* Corresponding author at: Meiji Institute for Advanced Study of Mathematical Sciences, Meiji University, 4-21-1 Nakano, Nakano-ku, Tokyo 164-8525, Japan. Tel.: +81 08047360992.

¹ Permanent address: Department of Mathematics, Jahangirnagar University, Savar, Dhaka - 1342, Bangladesh. Tel.: +88 01712280992. E-mail address: osmanganiju@gmail.com, gani@meiji.ac.jp (M.O. Gani).

is capable of improving the shape of the cardiac action potential [19]. The action potential of a cardiac cell (myocardium) has four different phases: resting membrane potential, rapid depolarization, plateau, and rapid repolarization. The cardiac action potential mainly differs from the neuronal action potential in terms of the duration of the action potential or plateau phase. In a nerve cell the action potential duration is approximately 1 ms. However, the cardiac action potential has a prolonged plateau phase lasting around 300 ms [30]. Previous studies [31–36] of the Aliev–Panfilov model focused on investigating only the spiral wave instability or the spiral chaos in two-dimensional numerical simulations. In the context of cardiac electrical activities, the spiral breakup phenomenon is known as ventricular fibrillation. Spiral waves are of course two-dimensional, but they become one-dimensional as one moves away from the center of the medium. A spiral wave approaches a periodic traveling wave solution at a sufficiently large distance from the center. Instability of the PTW will lead to spiral instability, and therefore, possible spiral breakup. To the best of our knowledge, no published work has investigated the stability of periodic traveling wave solutions in the Aliev–Panfilov model.

Thus, the aim of this paper is to study the stability of PTWs in the Aliev–Panfilov model, which is given by (1) and (2) later in the paper. We establish the existence and stability of the PTW solutions of the model in a two-dimensional parameter plane. This is done by the method of continuation via the continuation package WAVETRAIN [18]. It is observed that a PTW solution loses its stability in the model through a stability change of Eckhaus type. The family of PTWs with constant period crosses the stability boundary, and the waves bifurcate to an oscillating wave pattern. We also study the existence and stability of the PTWs as a function of the parameter b in (2), which is responsible for creating gaps between two nullclines at the right slow manifold. Moreover, we show stable and unstable spiral dynamics in model (2) in a one-parameter family of solutions.

The remainder of the paper is organized as follows. In Section 2, we describe the models and methods of computation. In Section 3, we present and discuss the results in one and two dimensions. Finally, we conclude the paper in Section 4.

2. Methods

2.1. Model

2.1.1. Original

The Aliev–Panfilov model [19] consists of two equations describing the fast and slow dynamics of an excitable medium, and it is given as follows:

$$\begin{aligned} \frac{\partial u}{\partial t} &= d_u \Delta u + ku(1-u)(u-a) - uv, \\ \frac{\partial v}{\partial t} &= d_v \Delta v + \epsilon(u, v)(ku(1+a-u) - v), \end{aligned} \tag{1}$$

where $\epsilon(u, v) = \epsilon_0 + \mu_1 v / (u + \mu_2)$ and the reaction terms $f(u, v) = ku(1-u)(u-a) - uv$ and $g(u, v) = \epsilon(u, v)(ku(1+a-u) - v)$ describe the local kinetics of variables u and v . The parameter ϵ , $0 < \epsilon \ll 1$, describes the ratio of the time scales of variables u and v . The fast activator variable u and the slow inhibitor variable v are known as the excitable and recovery variables, respectively. They are also referred to as the propagator and controller variables, respectively. The nullclines ($f(u, v) = 0, g(u, v) = 0$) of (1) has been plotted in [19]. The u -nullcline ($u_t = 0$) is N -shaped, as in the case of the standard FHN model [14,15]. However, the Aliev–Panfilov uses the term uv instead of v in the first equation of the FHN model. This improves the shape of the cardiac action potential. The v -nullcline ($v_t = 0$) is not linear or monotone as in the FHN model, but it is quadratic. This type of nullcline geometry is more appropriate for the cardiac cell dynamics [19]. The parameter a is called the threshold. It lies between 0 and 1/2, i.e., $0 < a < 1/2$. For a small perturbation of u less than the threshold value, i.e., $u < a$, the system reverts to the rest state; otherwise (i.e., $u > a$), the system undergoes long excursions with fast-slow dynamics in the (u, v) -plane before reverting to the stationary or $(0, 0)$ state. Therefore, the system is an excitable system [37].

2.1.2. Modified

In this paper, we use the following variant of the Aliev–Panfilov model in order to control the distance between the two nullclines uniformly at the right branch (marked by “R” in Fig. 1(a)) of the uv -plane as reported in [17,38].

$$\begin{aligned} \frac{\partial u}{\partial t} &= d_u \Delta u + ku(1-u)(u-a) - uv, \\ \frac{\partial v}{\partial t} &= d_v \Delta v + \epsilon(u, v)(du(1+b-u) - v). \end{aligned} \tag{2}$$

In (2), there are two new parameters d and b instead of k and a , respectively, in the second equation of (1). As a result, we can slow down the solution profile on the slow manifold at the right branch by taking the value of b as small as required. The nullclines of (2) are plotted in Fig. 1(a). Both nullclines intersect each other at a point that is called the rest state of the excitable medium. The point corresponds to the $(0, 0)$ state as shown in Fig. 1(a). Thus, there exists only one possible steady-state solution. The parameter b in (2) is responsible for the creation of gaps between the two nullclines at the right knee or branch of the uv -plane. It plays a crucial role in the model. Specifically, it controls the period of excitation of the medium and can have any value greater than 0, because the two nullclines intersect each other at the right knee when $b = 0$. The excitation period increases as b approaches 0 and decreases as b increases. This is crucial for controlling the velocity of the solution at the right slow manifold,

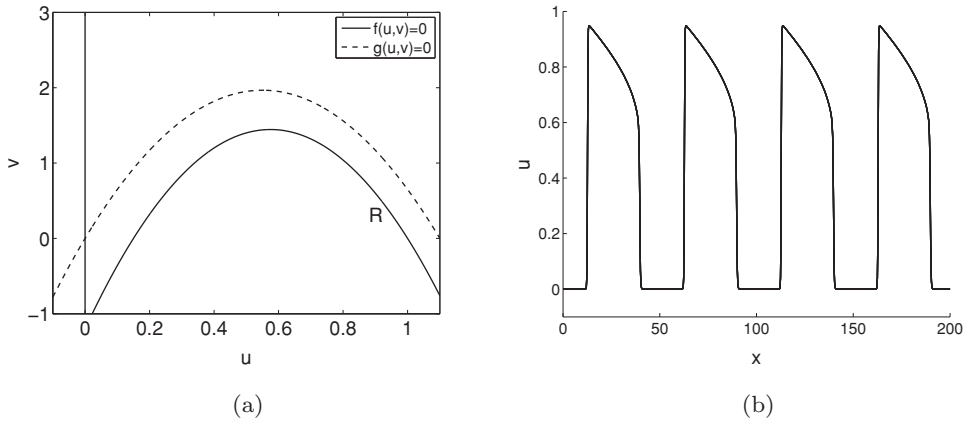


Fig. 1. (a) Nullclines of model (2) for $a = 0.15$, $k = 8.0$, $d = 6.5$, and $b = 0.1$. (b) A direct numerical solution (pulse profile) of (2) with $\epsilon_0 = 0.002$, $a = 0.15$, $k = 8.0$, $d = 6.5$, $\mu_1 = 0.2$, $\mu_2 = 0.3$, $b = 0.1$, $d_u = 0.05$, $d_v = 0.005$, and system size $L_x = 200$.

as compared to the original Aliev–Panfilov model (1). The parameter d is responsible for adjusting the height of the v -nullcline. The value of d is important for achieving a uniform gap between the two nullclines at the right branch. In this paper, d is fixed at $d = 6.5$. Our aim is to understand the stability of periodic traveling wave solutions in (2) as a function of the parameter b and the wave speed c . In general, it is difficult to understand the stability of PTWs of a PDE. The first step is to perform numerical simulations of the whole PDE. For example, a numerical simulation of (2), shown in Fig. 1(b), indicates a stable PTW of the model. We used an implicit scheme with periodic boundary conditions on $[0, L_x]$. Numerical integration was performed with space step $dx = 0.2$ and time step $dt = 0.01$ on a domain of size $L_x = 200$.

2.2. Review of theoretical results

We look for the solutions of (1) in one spatial dimension with fixed shape and wave speed: $u(x, t) = U(z)$, $v(x, t) = V(z)$, and $z = x - ct$, where x and t are the space and time coordinates, respectively, and c is the wave speed. In this moving coordinate system, the equations in (1) reduce as follows:

$$\begin{aligned} d_u U_{zz} + cU_z + f(U, V) &= 0, \\ d_v V_{zz} + cV_z + g(U, V) &= 0. \end{aligned} \tag{3}$$

Reducing to the first order, the above system (3) becomes

$$\begin{aligned} \frac{dU}{dz} &= P, \\ \frac{dP}{dz} &= (-cP - kU(1-U)(U-a) + UV)/d_u, \\ \frac{dV}{dz} &= Q, \\ \frac{dQ}{dz} &= (-cQ - \epsilon(U, V)(kU(1+a-U) - V))/d_v. \end{aligned} \tag{4}$$

A periodic traveling wave solution $(U(z), V(z))$ is a periodic orbit of this ordinary differential equation (ODE) system (4). In order to study the stability of periodic traveling wave solutions, it is convenient to reformulate (1) in terms of z and t , i.e., $u(x, t) = \tilde{u}(z, t)$ and $v(x, t) = \tilde{v}(z, t)$. Then, (1) becomes

$$\begin{aligned} \frac{\partial \tilde{u}}{\partial t} &= c \frac{\partial \tilde{u}}{\partial z} + d_u \frac{\partial^2 \tilde{u}}{\partial z^2} + f(\tilde{u}, \tilde{v}), \\ \frac{\partial \tilde{v}}{\partial t} &= c \frac{\partial \tilde{v}}{\partial z} + d_v \frac{\partial^2 \tilde{v}}{\partial z^2} + g(\tilde{u}, \tilde{v}). \end{aligned} \tag{5}$$

The linearization of the co-moving frame reaction–diffusion Eq. (1) about the steady state $(U(z), V(z))$, by using $\tilde{u}(z, t) = \underline{u}(z, t) + \hat{U}(z, t)$, is given by

$$\frac{\partial \hat{U}}{\partial t} = c \frac{\partial \hat{U}}{\partial z} + D \frac{\partial^2 \hat{U}}{\partial z^2} + \mathbf{J}_F \cdot \hat{U} = \mathcal{L} \hat{U}, \tag{6}$$

where \mathbf{J}_F denotes the Jacobian matrix of $(f(\tilde{u}, \tilde{v}), g(\tilde{u}, \tilde{v}))$ with respect to \tilde{u} and its derivative along the periodic traveling wave, and $D = \text{diag}(d_u, d_v)$ is the diffusion matrix. The linear operator \mathcal{L} is defined as

$$\mathcal{L} := c \frac{\partial}{\partial z} + D \frac{\partial^2}{\partial z^2} + \mathbf{J}_F. \tag{7}$$

Spectral stability of the wave ($U(z), V(z)$) can be determined by the spectrum of the linearized operator \mathcal{L} . The eigenvalue problem of (6) is given by

$$\lambda \hat{\phi} = c \frac{d}{dz} \hat{\phi} + D \frac{d^2}{dz^2} \hat{\phi} + \mathbf{J}_F \cdot \hat{\phi} = \mathcal{L} \hat{\phi}, \tag{8}$$

with the appropriate boundary conditions derived using Floquet theory [39–41] are given by

$$\hat{\phi}(L) = \hat{\phi}(0) \exp(i\gamma), \text{ for some } \gamma \in \mathbb{R}, \tag{9}$$

where L is the period of the PTW, γ is the phase shift across one period of the wave, $\hat{\phi}$ is the eigenfunction, and λ is the eigenvalue. The stability of the PTWs or the calculation of essential spectra depends essentially on the boundary conditions (9). Thus, the boundary conditions are crucial. Using the method adopted in [40], WAVETRAIN determines the stability of a PTW by calculating the essential spectrum via the continuation technique. A spectrum $\lambda(\gamma)$ of a PTW solution is the set of all eigenvalues λ such that (8) and (9) have a non-trivial solution [18]. For $\gamma = 0$, (8) and (9) can be solved by standard numerical methods. However, when $\gamma \neq 0$, these equations cannot be reduced to a matrix eigenvalue problem; hence, WAVETRAIN applies the numerical continuation method to the phase difference γ [18] for the calculation of essential spectra. In this case, one first needs to calculate matrix eigenvalues and the corresponding eigenfunctions for $\gamma = 0$ and use these solutions as initial data for the continuation over $0 < \gamma < 2\pi$ for some selected matrix eigenvalues near the imaginary axis. For this purpose, one first needs to write (8) as a first-order ODE system, which is given by

$$\frac{d\underline{v}}{dz} = (A(z) + \lambda B)\underline{v}. \tag{10}$$

Here, $\underline{v}(z) \in \mathbb{R}^4$, the matrices A and B are of size 4×4 , and $A(z)$ is periodic with period L . Now, in order to rescale L to unity and to get the appropriate boundary conditions for the continuation, one needs to consider the following Bloch transformation [40,42]:

$$\underline{v}(z) = e^{\frac{i\gamma z}{L}} \underline{w}(z), \text{ where } \zeta = \frac{z}{L}. \tag{11}$$

Therefore, (10) reduces to the following form:

$$\frac{d\underline{w}}{d\zeta} = L[A(\zeta) + \lambda B]\underline{w} - i\gamma \underline{w}, \quad \underline{w}(1) = \underline{w}(0). \tag{12}$$

For each $v = i\gamma \in \mathbb{C}$, the Bloch-wave operator [40] is given by

$$\mathcal{L}_v := c \left(\frac{\partial}{\partial z} + v \right) + D \left(\frac{\partial}{\partial z} + v \right)^2 + \mathbf{J}_F. \tag{13}$$

Further, (12) represents a first-order ODE system of the following original eigenvalue problem:

$$\lambda \hat{\psi} = \mathcal{L}_v \hat{\psi}, \quad \hat{\psi}(1) = \hat{\psi}(0). \tag{14}$$

Thus, one can calculate the essential spectra of the linearized operator \mathcal{L} by continuing some selected eigenvalues λ of the Bloch-wave operators \mathcal{L}_v defined in (13) in the parameter γ [40].

2.3. The WAVETRAIN package

We used the continuation package WAVETRAIN [18] for studying the PTWs. WAVETRAIN is a software for the study of PTWs of PDEs, which uses AUTO [43] to perform continuation of solutions. Solving the above equations in (12) requires several special settings, such as integral constraints to ensure the normalization of the rescaled eigenfunction and set orthogonality conditions (full details are given in [40]). WAVETRAIN [18] manages all these settings to solve the original Eqs. (8) and (9). In order to understand the stability of the PTW solutions, we need to calculate the spectra of the PTWs. In general, the spectra of linear operators consist of two parts: a discrete part and a continuous part. These two parts are known as the point spectrum and the essential spectrum, respectively. However, for PTWs, the point spectrum is always empty [41]. Therefore, the spectrum of a PTW solution in a large domain consists of only the essential spectrum [41,42]. A PTW solution is said to be stable if the essential spectrum of the solution does not cross the imaginary axis; otherwise, it is unstable [42]. If the curvature of the spectrum of a PTW solution changes sign at the origin, then the PTW has instability of Eckhaus type. However, if a fold is generated in the curvature of the spectrum and crosses the imaginary axis away from the origin, then it is called a stability change of Hopf type [42]. The necessary conditions for the stability change of a PTW solution of Eckhaus type are

$$\lambda = \operatorname{Re} \left(\frac{d\lambda}{d\gamma} \right) = \operatorname{Re} \left(\frac{d^2\lambda}{d\gamma^2} \right) = 0,$$

whereas a stability change of Hopf type occurs when

$$\operatorname{Re}(\lambda) = \operatorname{Re} \left(\frac{d\lambda}{d\gamma} \right) = 0 \text{ with } \operatorname{Im}(\lambda) \neq 0.$$

However, for the sufficient condition one needs to add a transversality condition, i.e., the derivative of $\operatorname{Re}(\lambda)$ with respect to the parameter γ is non-zero (for full details, we refer to [18,42]).

2.4. Numerical methods for PDE integration

For direct numerical simulations in one dimension, we used an implicit scheme with periodic boundary conditions on $[0, L_x]$. For numerical computations in two dimensions, we used the alternating direction implicit (ADI) method [44,45] with Neumann boundary conditions.

3. Results and discussion

3.1. Stability of PTWs in the original Aliev–Panfilov model

In this section, we study the stability of PTWs of (1). We used a numerically calculated periodic orbit from the PDEs as an initial solution for the continuation. Fig. 2(a) shows the existence and stability of the PTWs of (1) as a function of the threshold parameter a and the wave speed c . The other parameters are the same as those listed in Table 1. In [46], the parameter a is important for determining the spiral wave instability in two spatial dimensions. We consider a sufficiently small diffusion coefficient for the second component instead of zero, because in this case, the traveling wave ODEs (4) are more regular. The triangles on the parameter plane indicate that there is no PTW solution at that point, and the circles indicate the existence of PTWs. The green line represents the stability boundary of Eckhaus type between stable and unstable PTWs. For the mathematical details of the Eckhaus instability, we refer to [40], and for the calculation procedure of the stability boundary, we refer to [42]. The red (blue) circles indicate stable (unstable) PTWs at a given point of the wave speed c and the parameter a . The gray line is the locus of the PTWs with constant period = 25. Let us call this line the “iso-period” line. We observe that the iso-period line crosses the Eckhaus stability boundary. This stability information is important for determining spiral instability in two spatial dimensions in the numerical simulation later in the paper. The point where eigenvalues cross the imaginary axis is seen at the level of an extended medium as the emergence of spontaneous oscillations. We also observe that the waves having sufficiently small periods are always unstable [1,24]. Fig. 2(b) shows a bifurcation diagram for $a = 0.1$, which calculates the wave period as a function of wave speed. Plotting the wave period as a function of the wave speed is a standard way of presenting PTW families, which is known as the dispersion relation of the PTWs. In the dispersion curve, the fast ($c > 0.1815$) and slow ($c < 0.1815$) branches are connected at a critical point ($c_0 = 0.1815, L_0 = 2.90$), where the wave period has a local minimum value (see Fig. 2(b)). The Eckhaus bifurcation point between stable and unstable PTWs is at $c_E = 0.2952$ and $L_E = 6.76$. This indicates the onset of the instability of the PTWs. Thus, the PTWs having period less than 6.76 are always unstable in the fast branch. The slow branch is always unstable [40]. We

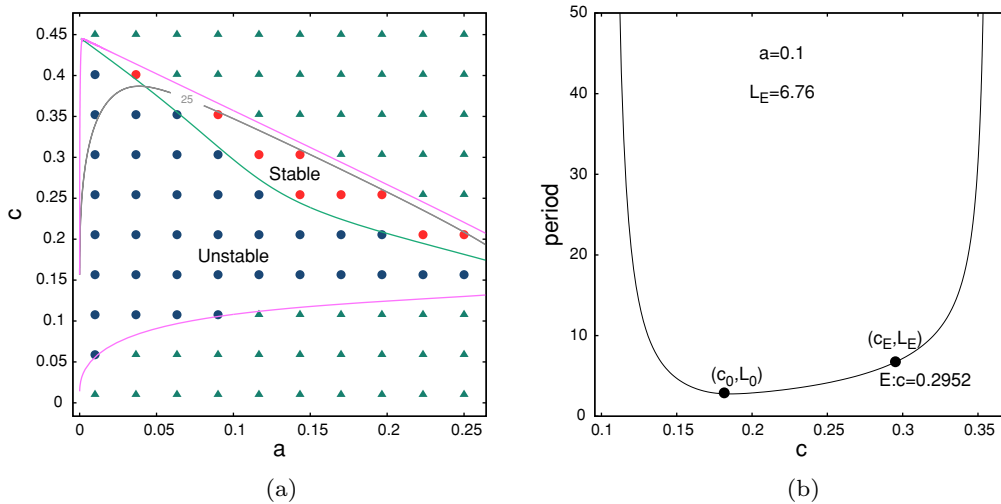


Fig. 2. PTW stability in the original Aliev–Panfilov model. (a) Existence and stability of PTWs of (1) as a function of a and c . The parameter values are the same as those listed in Table 1. The symbols represent the results on a 10×10 grid in the parameter plane: \blacktriangle indicates that there is no PTW at that point; \bullet indicates the existence of a stable PTW; \circ indicates the existence of an unstable PTW. The green solid line is the Eckhaus-type stability boundary between stable and unstable PTWs. The gray line is the locus of the PTWs with constant period = 25. The pink lines are the loci of homoclinic solutions. (b) The branch of the PTWs (or the bifurcation diagram) of (1) when a is fixed at $a = 0.1$. The curves were calculated and plotted using the software package WAVETRAIN [18]. (For interpretation of the references to color in this figure legend, the reader is referred to the web version of this article.)

Table 1
Typical set of parameter values in (1) used in the numerical computation [19].

Parameters	k	a	μ_1	μ_2	d_u	d_v	ϵ_0
Values	8.0	...	0.2	0.3	0.05	0.005	0.002

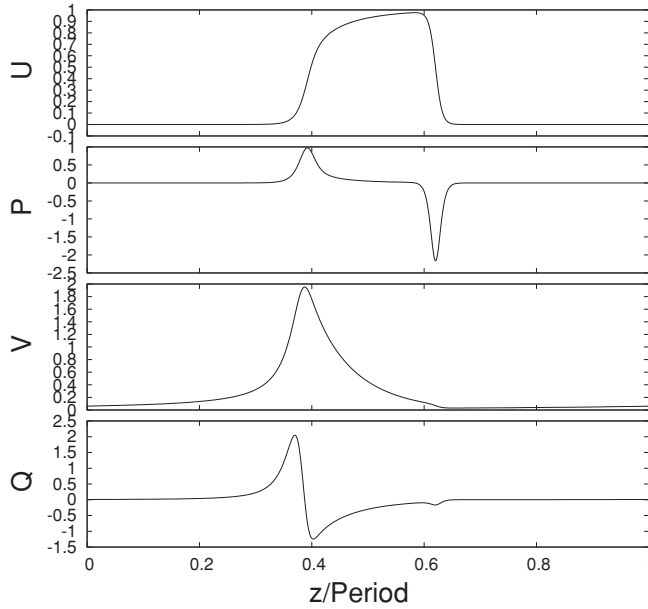


Fig. 3. A periodic traveling wave solution of (1). $U, P, V,$ and Q are the internal names of state variables; refer to Eq. (4). In this case, $a = 0.15$ and $c = 0.3$. The period of the PTW is 19.43. The other parameter values are the same as those listed in Table 1.

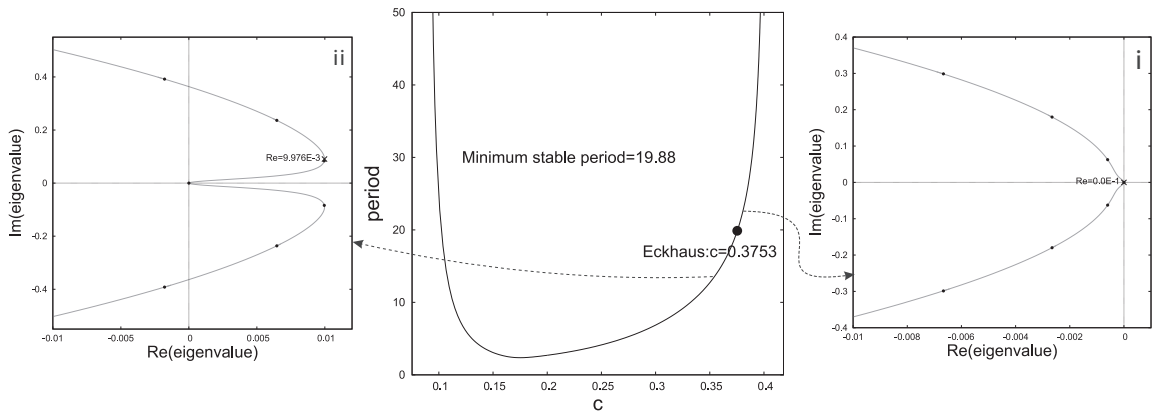


Fig. 4. In the center: a bifurcation diagram of the PTWs for $a = 0.05$. The plots (i) and (ii) illustrate the essential spectra for different parts of the dispersion curve. The gray lines indicate the spectra and the black dots denote eigenvalues corresponding to eigenfunctions for $\gamma = 0$ in (9). The essential spectra are for (i) a stable PTW, when $c = 0.376$ and $a = 0.05$, and (ii) an unstable PTW, when $c = 0.36$ and $a = 0.05$.

show this phenomenon by calculating the essential spectrum later in the paper, as shown in Fig. 4. Fig. 2(b) also shows that as the period of these PTWs approaches a very large value, their velocities approach a limiting wave speed and the waves approach a homoclinic solution. Thus, the PTW branches (families) begin and end at homoclinic solutions (see Fig. 2(b)). It is possible to calculate actual locus of homoclinic solutions by numerical continuation [47,48]. However, it is easier to approximate the locus by a PTW solution of a large period (say, 1000). Fig. 2(b) also indicates that the region giving waves in Fig. 2(a) is bounded above and below by the locus of homoclinic solutions. We find that if the PTWs exist for a parameter setting of the PDEs, then they also exist for a range of the wave speed c [1]. Fig. 3 shows the profile of a solution in the (a, c) -parameter space, where the parameter $a = 0.15$ and the wave speed $c = 0.15$. The corresponding period of the PTW is 19.43.

Fig. 4 shows the essential spectra of the PTWs for different parts of a dispersion curve. The central plot of Fig. 4 is a dispersion curve for $a = 0.05$. This curve shows fast and slow PTW branches. The fast ($c > 0.17$) and slow ($c < 0.17$) wave branches are connected by the critical point at $L_0 = 2.4$ and $c_0 = 0.17$. Plot (i) shows an essential spectrum of a stable PTW of (1), when the wave speed $c = 0.376$. It corresponds to a PTW at the fast branch before the Eckhaus bifurcation point ($c > 0.3753$). The Eckhaus bifurcation point is at $c_E = 0.3753$, where the onset of PTW instability occurs. The period at the Eckhaus bifurcation point is $L_E = 19.88$, which is the minimum stable period of the PTWs. The spectrum is located in the left half of the complex plane, meaning that the PTW is stable. Plot (ii) shows an essential spectrum of an unstable PTW, when the wave speed $c = 0.36$, which corresponds to a PTW after the Eckhaus bifurcation point ($c < 0.3753$). In this case, the curvature of the spectrum crosses the

Table 2
Typical values for the parameters in (2) used in the computation.

Parameters	k	d	a	b	μ_1	μ_2	d_u	d_v	ϵ_0
Values	8.0	6.5	0.15	...	0.2	0.3	0.05	0.005	0.002

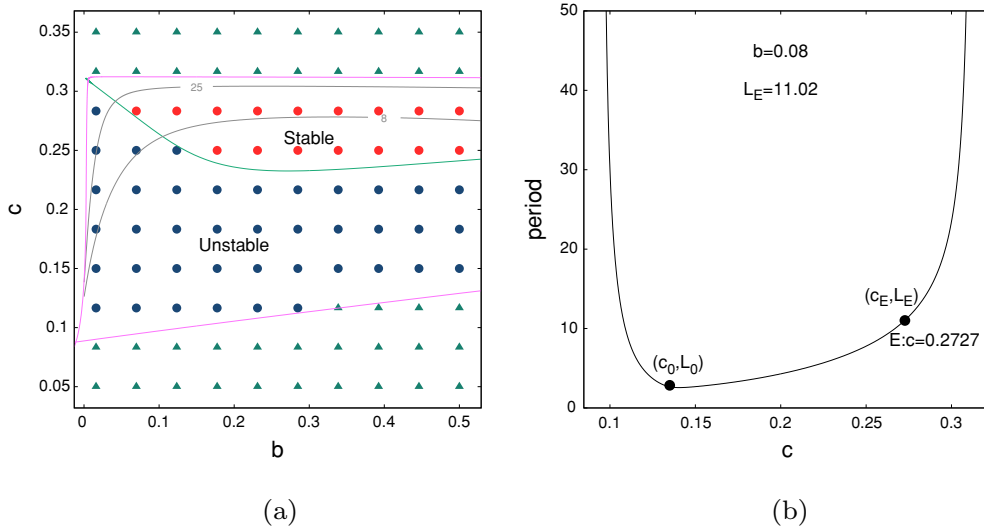


Fig. 5. (a) Existence and stability of PTWs of (2) as a function of b and c . The parameter values are the same as those listed in Table 2. The symbols represent the results on a 10×10 grid in the parameter plane: \blacktriangle indicates that there is no PTW at that point; \bullet indicates the existence of a stable PTW; \bullet indicates the existence of an unstable PTW. The green line is the Eckhaus-type stability boundary between stable and unstable PTWs. The gray lines are the loci of the PTWs with constant periods. The pink lines are the loci of homoclinic solutions. (b) The branch of the PTWs (or dispersion curve) of (2) when b is fixed at $b = 0.08$. (For interpretation of the references to color in this figure legend, the reader is referred to the web version of this article.)

imaginary axis at zero, meaning that the PTW has instability of Eckhaus type. Therefore, we conclude that the waves are unstable beyond the Eckhaus bifurcation point ($c < 0.3753$).

3.2. Stability of PTWs in a variant of the Aliev–Panfilov model

In this section, our aim is to determine the existence and stability of PTWs of (2). Here, we consider the parameter b as a control parameter, while the other parameters are the same as those listed in Table 2. The parameter b is important because it determines the gap between the two nullclines at the right branch, as mentioned earlier. The meanings of the symbols in the parameter plane are the same as in Fig. 2. The gray lines are the loci of the PTWs with constant periods = 25 and 8. We observe that the iso-period lines cross the Eckhaus stability boundary as b decreases. The blue circular points below the stability boundary indicate that the waves having sufficiently small periods are unstable [1,24]. Fig. 5(b) shows a dispersion curve for the parameter $b = 0.08$. The Eckhaus (E) bifurcation point between stable and unstable PTWs is at $(0.2727, 11.02)$. The PTWs are also unstable between the Eckhaus point (c_E, L_E) and the critical point $(c_0, L_0) = (0.135, 2.85)$ in the fast family. Thus, the PTWs having periods less than 11.02 are always unstable in the fast branch. Fig. 5(b) also shows that the PTW branches (families) begin and end at homoclinic solutions. This indicates that the region giving waves in Fig. 5(a) is bounded above and below by the homoclinic solutions. The pink lines are the loci of the homoclinic solutions (see Fig. 5(a)). The main advantage of the model (2) is that the stability boundary is nearly parallel to the iso-period lines for $b \geq 0.2$. This suggests that the periods of the PTWs are constant even we increase the gap between the two nullclines. However, for $b < 0.2$, the stability boundary gradually becomes steeper under change of b (see Fig. 5(a)). As a result, the iso-period lines cross the stability boundary.

In Fig. 6, we calculate the essential spectra of the PTWs for different parts of a dispersion curve of the model (2). The central plot of Fig. 6 is a dispersion curve for $b = 0.05$. Plot (i) shows an essential spectrum of a stable PTW of (2), when the wave speed $c = 0.29$, which corresponds to a PTW at the fast branch before the Eckhaus bifurcation point ($c > 0.2875$). The minimum stable period at the Eckhaus bifurcation point is $L = 20.02$. The spectrum is located in the left half of the complex plane, meaning that the PTW is stable. This suggests that for all PTWs in the fast branch for $c > 0.2875$, the eigenvalues have a negative real part. Plot (ii) shows an essential spectrum of an unstable PTW, when the wave speed $c = 0.28$, which corresponds to a PTW after the Eckhaus bifurcation point ($c < 0.2875$). The spectrum crosses the imaginary axis, meaning that the eigenvalues have a positive real part and the PTW is unstable. Thus, the PTWs in the fast branch having sufficiently large periods between the Eckhaus point and the critical point are also unstable in the modified Aliev–Panfilov model (2).

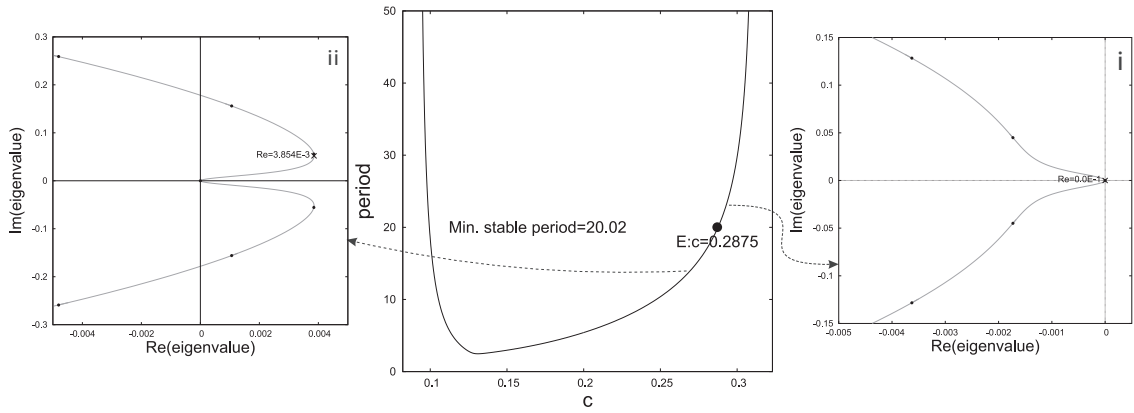
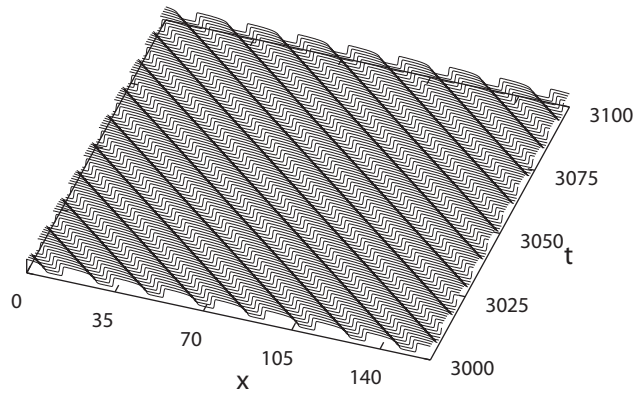
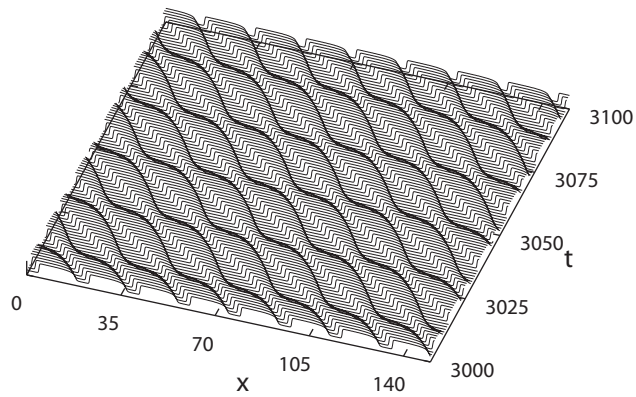


Fig. 6. In the center: a bifurcation diagram (or dispersion relation) of the PTWs for $b = 0.05$. The plots (i) and (ii) illustrate the essential spectra for different parts of the dispersion curve. The gray lines indicate the spectra and the black dots denote eigenvalues corresponding to eigenfunctions for $\gamma = 0$ in (9). The essential spectra are for (i) a stable PTW, when $c = 0.29$ and $b = 0.05$, and (ii) an unstable PTW, when $c = 0.28$ and $b = 0.05$.



(a)



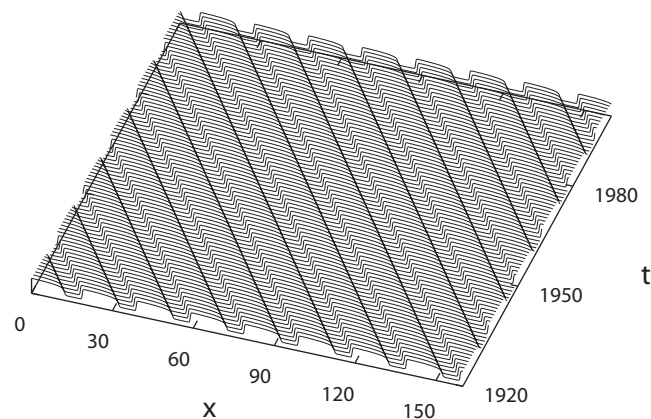
(b)

Fig. 7. Space-time plots of the PTWs in the PDE simulation of (1) based on the dispersion curve in Fig. 4 (center plot). The parameter settings are the same as in Fig. 4. (a) A stable PTW for the system size $L_x = 160$ (i.e., spatial period $l_1 = 20$). (b) An “oscillating PTW” for the system size $L_x = 150$ (i.e., spatial period $l_2 = 18.75$).

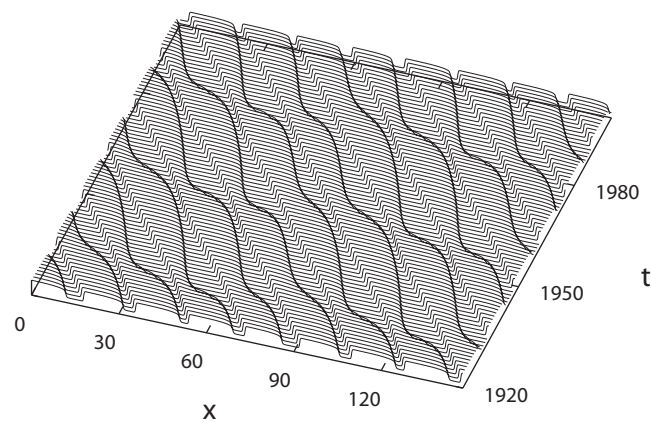
3.3. Oscillating PTWs through PDE simulations

In this section, we compare the results obtained in the previous sections with those of the corresponding direct PDE simulations. Fig. 7 shows different patterns of the PTWs in the PDE simulation around the Eckhaus bifurcation point. We used an implicit scheme with periodic boundary conditions on $[0, L_x]$. Numerical integration was performed with space step $dx = 0.166$ and time step $dt = 0.01$ on a grid of 960 elements. The parameter settings are the same as in Fig. 4. In Fig. 4, the dispersion curve shows that at the Eckhaus bifurcation point, the period of the PTW is $l = 19.88$. Therefore, we consider a PTW of eight pulses in a medium of system size $L_x = 160$, i.e., spatial period, say, $l_1 = 20$. The relation between the system size and the spatial period is defined as $L_x := n \times l$, where n is the number of pulses and l is the spatial period or wavelength. Fig. 7(a) shows a stable PTW solution for the system size $L_x = 160$, i.e., spatial period $l_1 = 20$, when $l_1 > l$. This period is slightly greater than the minimum stable period in Fig. 4 (center plot). We found an “oscillating PTW” in the simulation result. In Fig. 7(b), we consider a PTW of eight pulses in a system of length $L_x = 150$, i.e., spatial period $l_2 = 18.75$. Fig. 7(b) shows the “oscillating PTW” or alternans [49,50], when $l_2 < l$.

In Fig. 8, we compare the results of the stability change of the Eckhaus-type PTWs in model (2) with those of the simulations. The central plot in Fig. 6 shows a dispersion curve. A closer inspection reveals that the fast branch of the PTWs destabilizes



(a)



(b)

Fig. 8. Space-time plots based on the dispersion curve in Fig. 6 (central plot). (a) A stable PTW solution in the PDE simulation for $L = 161$ (i.e., $l_1 = 20.125$). (b) An “oscillating PTW” solution in the PDE simulation for $L = 148$ (i.e., $l_2 = 18.5$). The parameter settings are the same as in Fig. 6.

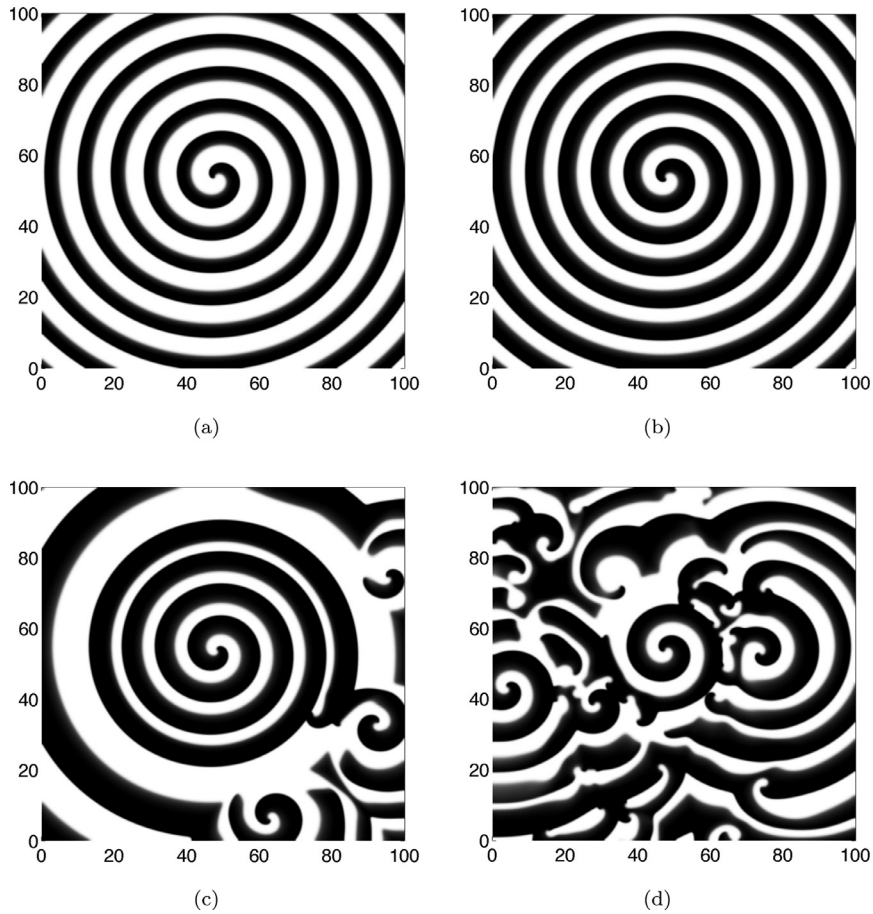


Fig. 9. The spiral wave dynamics as a function of b in (2). The other parameter values are the same as in Table 2 or Fig. 5. The panels are at (a) $b = 0.15$, (b) $b = 0.1$, (c) $b = 0.083$, and (d) $b = 0.08$. Numerical simulation with space step $dx = dy = 0.1$ and time step $dt = 0.02$ on a grid of 1000×1000 elements. The black area represents the excited state ($u = 1.0$) and the white area represents the resting state ($u = 0.0$) of the medium.

via a stability change of Eckhaus type when the wave speed $c = 0.2875$. We also observe that the minimum stable period of the PTWs at the Eckhaus point is approximately 20.02 (say, l). Now, we consider a PTW of eight pulses in a medium of system size $L_x = 200$. We gradually decreased the system size and found a stable pattern of solutions until the onset of the Eckhaus bifurcation. Fig. 8(a) shows a stable PTW solution for the system size $L_x = 161$, i.e., spatial period $l_1 = 20.125$, when $l_1 > l$. This period is slightly greater than the minimum stable period in Fig. 6. However, when we decreased the wavelength, we found an oscillatory pattern of solutions in a second simulation. Fig. 8(b) shows an “oscillating PTW” for the system size $L_x = 148$, i.e., spatial period $l_2 = 18.5$, when $l_2 < l$. Thus, the results of the traveling wave ODEs are consistent with the stability of the corresponding PDE simulation.

3.4. Spiral breakup phenomenon through PDE simulations

In this section, we present some simulation results in two dimensions of model (2) as a function of the parameter b . We considered the parameter b as a control parameter as a consequence of the one-dimensional numerical study. We found that the Eckhaus boundary in the (b, c) -parameter space becomes steeper as b decreases (see Fig. 5(a)). We would like to determine spiral instability for the same computational settings in this section.

First, Fig. 9 shows the dynamics of the spiral wave as a function of the parameter b of (2). We continued the simulation for a long time for every value of b in order to reach a steady-state solution. As an initial guess, we used a single traveling pulse solution truncated to half of the domain as a two-dimensional broken wave front in order to get the first initial spiral. Fig. 9(a and b) shows a stable spiral pattern for $b = 0.15$ and $b = 0.1$, respectively. The excited state (black area) becomes thicker in the second case as the parameter b decreases. The onset of instability or spiral breakup was found near the boundary of the medium for $b = 0.083$ (see Fig. 9(c)). The chaotic pattern increases when b is further decreased, and finally, far-field breakup is transmitted near the vicinity of the first initial spiral core with one initial pulse intact at around $b = 0.08$ (see Fig. 9(d)). These numerical results of the direct PDE simulations are consistent with the stability of the PTWs in the traveling wave ODEs presented in Fig. 5. Thus, the

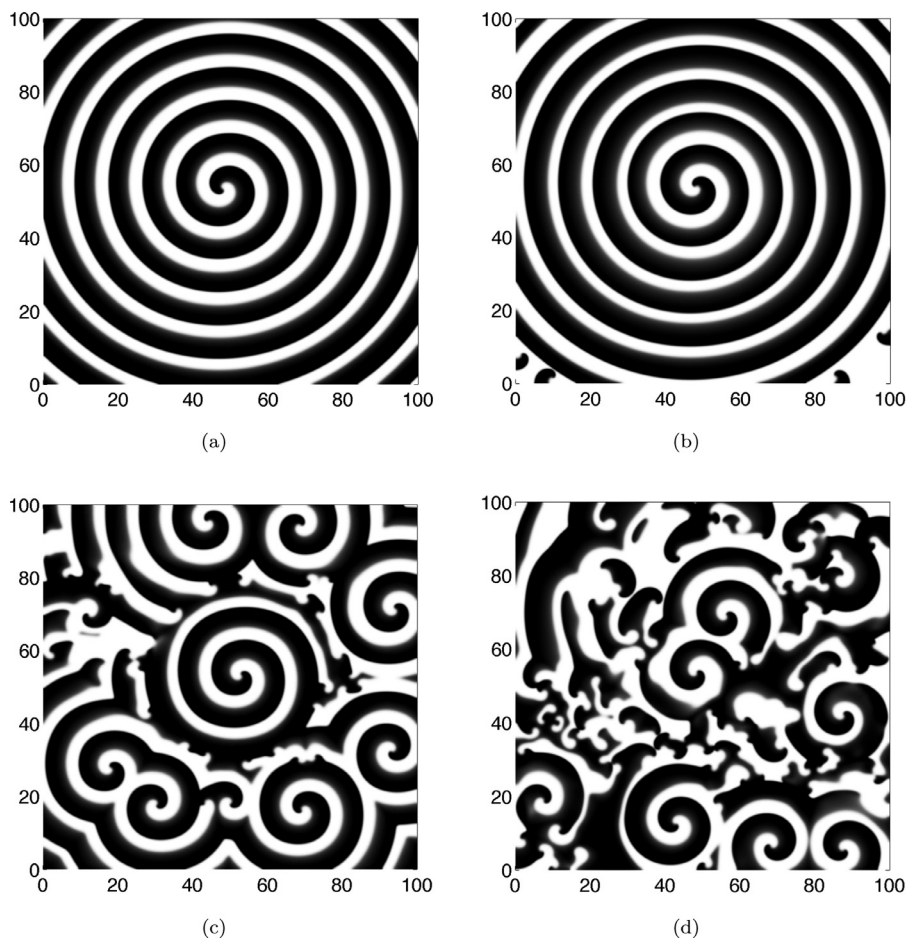


Fig. 10. Time sequence illustrating the dynamical mechanism of spiral breakup in (2) when $b = 0.08$. The other parameter values are the same as in Fig. 5. The panels are at (a) $t = 0$, (b) $t = 122$, (c) $t = 732$, and (d) $t = 1100$. Numerical simulation with space step $dx = dy = 0.1$ and time step $dt = 0.02$ on a grid of 1000×1000 elements.

spiral wave instability occurs as a consequence of the PTW instability. Several numerical studies related to spiral breakup in the Aliev–Panfilov model have been reported [19,34–36,51]. However, previous studies did not consider the parameter b as a control parameter in order to obtain stable and unstable spiral wave dynamics.

Next, we show the spiral breakup phenomenon of (2) as a function of time. Fig. 10 shows the evolution of spatial pattern formation when $b = 0.08$. Fig. 10(a) shows the dynamics of a stable spiral pattern, which is considered as an initial guess for the subsequent simulations in Fig. 10(b–d). Numerical integration is performed with space step $dx = dy = 0.1$ and time step $dt = 0.02$ on a grid of 1000×1000 elements. The parameter settings are the same as in Fig. 5(a). In this case, after several rotations of the spiral wave, the initial breakup occurs in the arm of the spiral wave (near the boundary) instead of the vicinity of the core (see Fig. 10(b)) at time $t = 122$. This type of breakup is known as far-field breakup [24]. Gradually, the excited state covered most regions of the medium. The pulse breaks at the spiral arm form two new spiral tips and make the medium spatially disorganized (see Fig. 10(c)). A new wave break produces two more new spirals. This process continues repeatedly throughout the medium, and at $t = 1100$, a chaotic pattern of waves appears (see Fig. 10(d)).

4. Conclusions

We studied the existence and stability of the periodic traveling wave solutions in an excitable reaction–diffusion system. In general, the PTWs exhibit stability change of either Eckhaus type or Hopf type [40]. The computational results obtained by the calculation of essential spectra confirmed Eckhaus-type instability in the original Aliev–Panfilov model and modified Aliev–Panfilov model. Our results showed that in PTWs, the stability change of Eckhaus type [42] occurs in waves having both small and large periods. The small-period waves are always unstable [1,24]. Therefore, the instability of the waves having large periods is important. We found in both models that the PTWs having large periods cross the stability boundary, and as a result, they bifurcate to an oscillating wave. The advantage of the modified Aliev–Panfilov model is that the excitation period increases as the parameter decreases (for a fixed value of the parameter a). Eventually, it reaches to a homoclinic solution (see Fig. 5(a)). Moreover,

the stability boundary becomes steeper as b decreases. As a result, the waves having large periods cross the stability boundary and bifurcate to an oscillating PTW. The oscillating periodic wave pattern was observed as a consequence of the Eckhaus bifurcation point (see Figs. 7 and 8). This indicates a good agreement between the continuation result of the traveling wave ODEs and the stability of the corresponding direct numerical simulation of the PDE system. The instability of the PTWs in one dimension is closely related to the instability of the spiral wave in two dimensions [46]. The determination of the mechanism of spiral instability or spiral breakup in cardiac activity is an open problem. Our two-dimensional results showed that the spiral instability is caused by the PTW instability in the modified Aliev–Panfilov model. Moreover, we found that far-field breakup [24] occurred as a consequence of the Eckhaus instability of the PTWs.

Conflict of interest

The authors declare that there is no conflict of interest regarding the publication of this paper.

Acknowledgments

This work is supported by the Global Center of Excellence (GCOE) program “Formation and Development of Mathematical Sciences Based on Modeling and Analysis”, Meiji University, Japan. We thank the anonymous reviewers for their insightful comments and suggestions that enabled us to improve the quality of the paper.

References

- [1] Kopell N, Howard LN. Plane-wave solutions to reaction-diffusion equations. *Stud Appl Math* 1973;52:291–328.
- [2] DeVille REL, Eijnden EV. Wavetrain response of an excitable medium to local stochastic forcing. *Nonlinearity* 2007;20(1):51–74.
- [3] Sherratt JA, Lord GJ. Nonlinear dynamics and pattern bifurcations in a model for vegetation stripes in semi-arid environments. *Theor Popul Biol* 2007;71(1):1–11.
- [4] Gani MO, Ogawa T. Alternans and spiral breakup in an excitable reaction-diffusion system: a simulation study. *Int Sch Res Not* 2014;2014:14.
- [5] Steinberg V, Fineberg J, Moses E, Rehberg I. Pattern selection and transition to turbulence in propagating waves. *Phys D: Nonlinear Phenom* 1989;37:359–83.
- [6] van Hecke M. Coherent and incoherent structures in systems described by the 1D CGL: experiments and identification. *Phys D: Nonlinear Phenom* 2003;174(1):134–51.
- [7] van Saarloos W. Front propagation into unstable states. *Phys Rep* 2003;386(2):29–222.
- [8] Epstein IR, Showalter K. Nonlinear chemical dynamics: oscillations, patterns, and chaos. *J Phys Chem* 1996;100(31):13132–47.
- [9] Vanag VK, Epstein IR. Design and control of patterns in reaction-diffusion systems. *Chaos: Interdiscip J Nonlinear Sci* 2008;18(2):026107.
- [10] Bordyugov G, Fischer N, Engel H, Manz N, Steinbock O. Anomalous dispersion in the Belousov–Zhabotinsky reaction: experiments and modeling. *Phys D: Nonlinear Phenom* 2010;239(11):766–75.
- [11] Ranta E, Kaitala V. Travelling waves in vole population dynamics. *Geochim Cosmochim Acta* 1997;61:3503–12.
- [12] Bierman SM, Fairbairn JP, Petty SJ, Elston DA, Tidhar D, Lambin X. Changes over time in the spatiotemporal dynamics of cyclic populations of field voles (*Microtus agrestis* L.). *Am Nat* 2006;167(4):583–90.
- [13] Sherratt JA, Smith MJ. Periodic travelling waves in cyclic populations: field studies and reaction–diffusion models. *J R Soc Interface* 2008;5(22):483–505.
- [14] FitzHugh R. Impulse and physiological states in theoretical models of nerve membrane. *Biophys J* 1961;1:445–65.
- [15] Nagumo JS, Arimoto S, Yoshizawa S. An active pulse transmission line simulating nerve axon. *Proc IRE* 1962;50:2061–71.
- [16] Karma A. Spiral breakup in model equations of action potential propagation in cardiac tissue. *Phys Rev Lett* 1993;71:1103–16.
- [17] Gani MO, Ogawa T. Instability of periodic traveling wave solutions in a modified FitzHugh–Nagumo model for excitable media. *Appl Math Comput* 2015;256:968–84.
- [18] Sherratt JA. Numerical continuation methods for studying periodic travelling wave (wavetrain) solutions of partial differential equations. *Appl Math Comput* 2012;218:4684–94.
- [19] Aliev RR, Panfilov AV. A simple two-variable model of cardiac excitation. *Chaos, Solitons Fractals* 1996;7:293–301.
- [20] Hodgkin AL, Huxley AF. A quantitative description of membrane current and its application to conduction and excitation in nerve. *J Physiol* 1952;117:500–44.
- [21] Bauer S, Röder G, Bär M. Alternans and the influence of ionic channel modifications: cardiac three-dimensional simulations and one-dimensional numerical bifurcation analysis. *Chaos: Interdiscip J Nonlinear Sci* 2007;17:015104.
- [22] Echebarria B, Röder G, Engel H, Davidsen J, Bär M. Supernormal conduction in cardiac tissue promotes concordant alternans and action potential bunching. *Phys Rev E* 2011;83:040902.
- [23] Sakaguchi H, Maruyama T. Elimination of pulses and spirals by external forces in Luo–Rudy model. *J Phys Soc Jpn* 2008;77:1–5.
- [24] Bär M, Brusch L. Breakup of spiral waves caused by radial dynamics: Eckhaus and finite wavenumber instabilities. *New J Phys* 2004;6:1–22.
- [25] Bordyugov G, Engel H. From trigger to phase waves and back again. *Physica D* 2006;215:25–37.
- [26] Bordyugov G, Engel H. Creating bound states in excitable media by means of nonlocal coupling. *Phys Rev E* 2006;74:016205.
- [27] Jonathan AS. History-dependent patterns of whole ecosystems. *Ecol Complex* 2013;14:8–20.
- [28] Sherratt JA. Pattern solutions of the Klausmeier model for banded vegetation in semiarid environments V: the transition from patterns to desert. *SIAM J Appl Math* 2013;73:1347–67.
- [29] Smith MJ, Sherratt JA. The effects of unequal diffusion coefficients on periodic travelling waves in oscillatory reaction-diffusion systems. *Physica D* 2007;236:90–103.
- [30] Pinnell J, Turner S, Howell S. Cardiac muscle physiology. *Contin Educ Anaesth Crit Care Pain* 2007;7(3):85–8.
- [31] Panfilov AV, Holden AV. Self-generation of turbulent vortices in a two-dimensional model of cardiac tissue. *Phys Lett A* 1990;147:463–6.
- [32] Panfilov AV, Holden AV. Spatio-temporal irregularity in a two-dimensional model of cardiac tissue. *Int J Bifurc Chaos* 1991;1:119–29.
- [33] Panfilov AV, Pertsov A. Ventricular fibrillation: evolution of the multiple-wavelet hypothesis. *Philos Trans R Soc Lond A* 2001;359:1315–25.
- [34] Panfilov AV. Spiral breakup as a model of ventricular fibrillation. *Chaos* 1998;8:57–64.
- [35] Zemlin CW, Panfilov AV. Spiral waves in excitable media with negative restitution. *Phys Rev E* 2001;63:041912.
- [36] Panfilov AV, Zemlin CW. Wave propagation in an excitable medium with a negatively sloped restitution curve. *Chaos: Interdiscip J Nonlinear Sci* 2002;12:800–6.
- [37] Meron E. Pattern formation in excitable media. *Phys Rep* 1992;218:1–66. (Review section of *Physics Letters*).
- [38] Nash MP, Panfilov AV. Electromechanical model of excitable tissue to study reentrant cardiac arrhythmias. *Prog Biophys Mol Biol* 2004;85(2):501–22.
- [39] Deconinck B, Nathan Kutz J. Computing spectra of linear operators using the Floquet–Fourier–Hill method. *J Comput Phys* 2006;219(1):296–321.
- [40] Rademacher JDM, Sandstede B, Scheel A. Computing absolute and essential spectra using continuation. *Physica D* 2007;229:166–83.
- [41] Sandstede B. Stability of travelling waves. *Handbook of dynamical systems II*. Fiedler B, editor. Amsterdam: North-Holland; 2002.p. 983–1055.

- [42] Sherratt JA. Numerical continuation of boundaries in parameter space between stable and unstable periodic travelling wave (wavetrain) solutions of partial differential equations. *Adv Comput Math* 2013;39:175–92.
- [43] Doedel EJ, Kernevez J. *AUTO: software for continuation and bifurcation problems in ordinary differential equations*. Pasadena, USA: California Institute of Technology; 1986. (Appl Math Rep).
- [44] Morton KW, Mayers DF. *Numerical solution of partial differential equations: an introduction*. Cambridge University Press; 2005.
- [45] Peaceman DW, Rachford HH Jr. The numerical solution of parabolic and elliptic differential equations. *J Soc Ind Appl Math* 1955;3(1):28–41.
- [46] Sakaguchi H, Fujimoto T. Elimination of spiral chaos by periodic force for the Aliev-Panfilov model. *Phys Rev E* 2003;67(6):067202.
- [47] Champneys AR, Kuznetsov YA. Numerical detection and continuation of codimension-two homoclinic bifurcations. *Int J Bifurc Chaos* 1994;4:785–822.
- [48] Champneys AR, Kuznetsov YA, Sandstede B. A numerical toolbox for homoclinic bifurcation analysis. *Int J Bifurc Chaos* 1996;6:867–87.
- [49] Courtemanche M, Glass L, Keener JP. Instabilities of a propagating pulse in a ring of excitable media. *Phys Rev Lett* 1993;70(14):2182.
- [50] Courtemanche M, Keener JP, Glass L. A delay equation representation of pulse circulation on a ring in excitable media. *SIAM J Appl Math* 1996;56(1):119–42.
- [51] Panfilov A, Hogeweg P. Spiral breakup in a modified FitzHugh-Nagumo model. *Phys Lett A* 1993;176:295–9.